Title

Physical Delivery of Macromolecules using High-Aspect Ratio Nanostructured Materials

Journal

ACS Applied Materials & Interfaces, 7(42)

ISSN

1944-8244

Authors

Lee, Kunwoo
Lingampalli, Nithya
Pisano, Albert P
et al.

Publication Date

2015-10-28

DOI

10.1021/acsami.5b05520

Peer reviewed

HHS Public Access

Author manuscript

ACS Appl Mater Interfaces. Author manuscript; available in PMC 2018 August 01.

Published in final edited form as:

ACS Appl Mater Interfaces. 2015 October 28; 7(42): 23387–23397. doi:10.1021/acsami.5b05520.

Physical Delivery of Macromolecules using High-Aspect Ratio Nanostructured Materials

Kunwoo Lee[†], **Nithya Lingampalli**[†], **Albert P. Pisano**[‡,§], **Niren Murthy**[†], and **Hongyun So**[‡,*]

[†]Department of Bioengineering, Berkeley Sensor & Actuator Center, University of California, Berkeley, California 94720, United States

[‡]Department of Mechanical Engineering, Berkeley Sensor & Actuator Center, University of California, Berkeley, California 94720, United States

[§]Jacobs School of Engineering, University of California, San Diego, California 92093, United States

Abstract

There is great need for the development of an efficient delivery method of macromolecules, including nucleic acids, proteins, and peptides, to cell cytoplasm without eliciting toxicity or changing cell behavior. High-aspect ratio nanomaterials have addressed many challenges present in conventional methods, such as cell membrane passage and endosomal degradation, and have shown the feasibility of efficient high-throughput macromolecule delivery with minimal perturbation of cells. This review describes the recent advances of in vitro and in vivo physical macromolecule delivery with high-aspect ratio nanostructured materials and summarizes the synthesis methods, material properties, relevant applications, and various potential directions.

Graphical Abstract

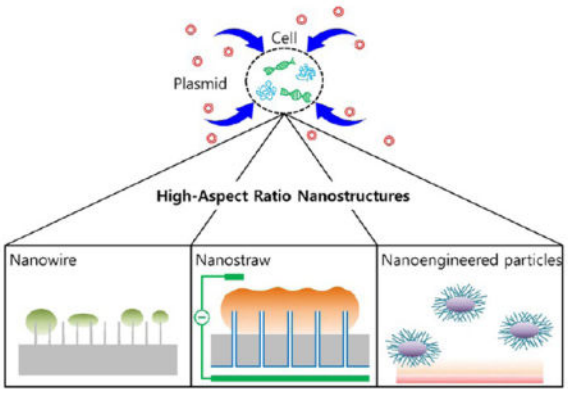

*Corresponding Author: hyso@berkeley.edu.

Notes

The authors declare no competing financial interest.

NOTE ADDED AFTER ASAP PUBLICATION

This paper was published on the Web on October 19, 2015, with a minor text error in the caption for Figure 6. The corrected version was reposted on October 28, 2015.

Keywords

high-aspect ratio; nanostructures; macromolecules; physical delivery; high-throughput

1. INTRODUCTION

The introduction of specific and controlled stimuli is a key for investigating and engineering biological systems. As a vital method for controlling cell stimuli, various biological effectors, including DNAs, RNAs, peptides, and proteins, require an efficacious delivery method.[1,2] Currently, the most widely utilized tools for the delivery of nucleic acids and proteins include biological methods, such as cell penetrating peptides and viruses, and chemical methods, such as cationic polymers and lipofectamine.[3–5] However, the challenges of delivery through the cell membrane and endosomal escape often limit the success of these methods.[5,6] As a result, there is a persistent and increasing demand in the field for efficient techniques of cellular macromolecule delivery.

As a method to avoid complicated cell membrane passage and endosomal degradation, direct physical delivery methods have been developed.[7,8] For example, microinjection using a glass micropipette to introduce molecules into individual cells has been widely used in biological sciences for decades. A microcapillary needle usually between 0.5 to 5 μm in diameter and stiff enough to penetrate the cell membrane is used for physical delivery.[9,10] The microinjection technique using physical penetration for intracellular delivery proves the effectiveness of macromolecule delivery.

Building on this finding, recent advancements in nanotechnology have miniaturized the needles and produced a variety of high-aspect ratio nanostructures that can deliver macromolecules to the cell cytoplasm without eliciting toxicity or altering cell behavior.[11,12] Many of the high-aspect ratio nanomaterials meet important criteria for an ideal biological reagent delivery method: (i) highly efficient delivery with minimal perturbation of cell function and viability, (ii) applicability to a wide variety of cell types, and (iii) ability to batch transfect.[2] Moreover, the design principle of high-aspect ratio nanostructures allows for a high-throughput approach and can be scaled up for batch applications by integration into microfluidic systems.[13] The invention of macromolecule delivery methods that can effectively introduce macromolecules into a variety of cell types in high-throughput has the potential to transform the field of biological and medical research.

The application of high-aspect ratio nanomaterials is not limited to in vitro systems, as there have been many approaches utilizing the interaction of high-aspect ratio nanostructures with various tissues to assist in macromolecule delivery.[10,14–16] For example, many nanostructures have achieved strong adhesion to a tissue surface and efficiently delivered various macromolecules. Figure 1 depicts a schematic illustration of both in vitro (Figure 1a) and in vivo (Figure 1b) macromolecule delivery applications by high-aspect ratio nanostructured materials, including nanowires, nanostraws, and nanoengineered particles. This review will discuss unique macromolecule delivery devices with high-aspect ratio nanofeatures, recent innovations in the design and synthesis of these devices, the underlying

mechanism of facilitated delivery, and a comparison of devices for in vitro and in vivo applications.

2. IN VITRO APPLICATIONS

2.1. Silicon Nanowires

Among the materials extensively studied for nanowire synthesis, silicon is especially distinguished due to its relatively high biocompatibility, a fact that establishes silicon nanowires (Si NWs) as an optimal candidate for macromolecule delivery. Si NWs can be synthesized to have a diameter between 5 and 100 nm, a few orders of magnitude smaller than the diameter of mammalian cells, which are ~10 μm. The high-aspect ratio and rigid structure of NWs allow for mechanical cellular delivery because of their direct access to the cytoplasm of living cells.[12] A study by Kim et al. shows that the physical interaction between high-aspect ratio NWs and cells allows the NWs to be introduced inside the cells.[12] Human embryonic kidney (HEK 293T) cells were cultured on prepared clusters of high-density NWs (90 nm diameter and 6 μm length). The cells were physically penetrated by high-aspect ratio Si NWs as they subsided in the culture medium. The physical interaction was visualized by confocal microscopy and scanning electron microscope (SEM) images. Figure 2a presents a confocal microscopy image of the NWs piercing the cells, represented by black dots inside the green fluorescent protein (GFP) expressing cells.[12] SEM images present that the individual cells were penetrated by Si NWs without the assistance of instrumentation or external forces. This is a pioneering research study that introduced the concept of nanostructure-induced cell penetration for delivery purposes. Although Kim et al. showed low delivery efficiency, further studies have improved the delivery efficiency and verified the technology in various model systems.[2,12,13]

The Park group tested the versatility of Si NWs with diverse macromolecular species in a variety of cell types.[2,13] Red fluorescent protein (RFP), mCherry, and dTomato expressing plasmid DNA have been effectively delivered via Si NWs to HeLa S3 cells and human fibroblasts, neuronal progenitor cells, and primary rat hippocampal neurons, respectively.[2] Macromolecules with fluorescence labeling, such as siRNA, peptides, plasmid DNA, and proteins, were successfully delivered to human fibroblasts (Figure 2c–f).[2] Additionally, the Park group applied Si NWs for mediated siRNA delivery to understand the mechanism of the Wnt signaling pathway in chronic lymphocytic leukemia.[13] The physical parameters of NWs were optimized for various primary immune cells that included bone marrow-derived dendritic cells (CD11c+), B cells (CD19+), dendritic cells (CD11c+), and T cells (CD4+).[13] Figure 3 demonstrates the contact of immune cells to Si NWs.[13] siRNA delivered using optimized NWs resulted in a substantial reduction of targeted mRNA levels up to 69%, and the expected phenotypic changes were successfully observed. Additionally, 3D DNA nanocages (DNA-NCs) were delivered using functionalized vertical silicon nanoneedle (Si NNs) arrays that were 1 μm in length and 100 nm in diameter.[17] Si NNs were aminosilane-functionalized Si NWs that can load DNA-NCs (7.65 nm in diameter) by noncovalent electrostatic interactions. HeLa S3 cells plated on top of the Si NN were physically penetrated, releasing the DNA-NCs into their cytoplasm. Functionalized DNA-NCs with organelle-localization signal peptides were observed to localize in target subcellular

compartments, such as mitochondria or the nucleus.[17] Co-localization was observed with confocal microscopy, and DNA-NCs had fluorescence signal overlaps with organelles, including mitochondria, nuclei stained with MitoTracker Green, or Hoechst 33342.[17] Nanoneedles made of porous Si also efficiently delivered quantum dots, siRNAs, plasmids, and bovine serum albumin (BSA) in HeLa cells.[9,10] Chiappini et al. showed that porous Si NNs placed on either the top or bottom of cells delivered quantum dots to the cells. Porous Si NNs placed on the bottom of a culture plate penetrated cell membrane of cells seeded over the needles. Furthermore, porous Si NNs placed on top of the seeded cells were able to penetrate the cell membrane from the top with force generated by centrifugation at 100 rcf for 1 min.[10]

Synthesis—The Si NWs can be grown using two distinct approaches: (1) bottom-up and (2) top-down. In the bottom-up approach, vapor–liquid–solid (VLS) growth by chemical vapor deposition (CVD) can synthesize epitaxially aligned single crystralline Si NWs. In the VLS process, catalysts such as a thin metal film or metal colloids are necessary to initiate the growth of the NW by triggering precipitation between catalyst and substrate materials at the eutectic temperature. The use of metal colloids provides well-dispersed and diameter-controlled Si NWs, whereas the fine control of the diameter is significantly more difficult when using thin metal films because of the randomness of the film shatterings at the reaction temperature.[18] For the vertical growth along the <111> direction, a (111) Si wafer can be used for epitaxial growth.[19,20] As a Si source (i.e., precursor molecule), $SiCl_4$ can be used in the CVD system. Finally, the growth on various substrates seeded with gold film or colloids can be conducted at high temperatures, between 800–1000 °C, for 1 h under the continuous flow of carrier gas.

In the top-down fabrication method of Si NWs, the pattern of the etching mask (usually thermally grown silicon oxide) on a Si wafer was followed by dry etching Si. Patterning of the protective mask can be achieved by either standard photolithography or nanosphere lithography with nanoparticle deposition.[21] Reactive-ion etching (RIE) was conducted following the formation of a patterning mask to uniformly and vertically etch the unprotected Si area.[22] As a result, the Si protected by the etching mask transforms to vertically aligned Si NWs.[2,13] The combination of top-down fabrication methods and metal-assisted chemical etching can be used for porous Si NNs.[9,10]

For nucleic acid delivery using the Si NW array, the DNA is deposited onto Si NW substrates by electrostatic forces. Binding is improved with polyethylenimine solution (PEI, 10% in water), a positively charged polymer that facilitates the deposition of negatively charged DNA.[12,23,24] The Park group achieved optimal loading of macromolecules by incubating Si NW substrates in 1% (v/v) 3-aminopropyltrimethoxysilane (APTMS) in toluene.[2] The Si NNs, which delivered 3D DNA-NCs, were based on Si NWs from the Park group[2] and were surface-functionalized with APTMS to bind negatively charged DNA-NCs.[17] Additionally, some approaches used the nano-needles functionalized with 2% (v/v) 3-aminopropyltriethoxysilane (APTES) in ethanol for nucleic acid delivery using the porous Si NNs.[9,10] One advantage of the Si nanotechnology is that the surface chemistry governing the external interactions of NWs is easily altered by a variety of chemical treatments, including

silanization. The wide range of inducible variability in NWs is highly favorable for the delivery of diverse macromolecules to a variety of cells.[2,13,15,25]

Cell Toxicity—Perturbation of some cell functions by NW penetration, such as reduced cellular growth, is inevitable. Annexin V binding analysis suggests that NW perturbation also causes lipid scrambling. However, many of the disturbed features observed after NW penetration were reversed once the cells cultured on NWs were detached by trypsin treatment and plated on culture plates or glass coverslips. Moreover, the cell culture on Si NWs over weeks did not significantly affect the growth and replication capabilities of the cells.[2,12] Additionally, primary rat hippocampal neurons displayed growth, development of synaptic connections, and functional firing of action potentials upon current injection, indicating normal physiological conditions.[2,13] Chan et al. conducted a live/dead assay with propidium iodide and trypan blue on HeLa cells after penetration and removal from the Si NNs to evaluate cytotoxicity of the system. Encouragingly, integrity of the cellular membrane was preserved, and 98% of the cells were viable after the delivery process.[17]

2.2. CNT and Carbon Nanostructures

Carbon nano-tubes (CNTs) or nanostructures can have a high-aspect ratio and rigidity, both features useful for the physical penetration of cells. The Bertozzi group developed a cell nanoinjector using a single multiwalled carbon nanotube (MWNT) attached to an atomic force microscope (AFM) tip.[5] A quantum dot was loaded onto the MWNT with a disulfide bond. An AFM cantilever was adjusted to contact the cell and finely controlled to penetrate the cell membrane. The MWNT nanoneedle was maintained inside the cell for a 15 to 30 min incubation period, a sufficient time interval for the cleavage of disulfide bonds and release of the quantum dot to occur.[5] Yum et al. also developed similar nanoinjection technology using a gold-coated nano-needle and demonstrated quantum dot delivery into living HeLa cells.[26] Although the delivery technique is highly accurate and effective, its application is limited to an individual cell, and it cannot be extended to multiple cell types concurrently. The widespread application is further restricted by its requirement of AFM.

Patterned carbon nanosyringe arrays (CNSAs) were designed to achieve simultaneous and efficient cellular delivery to multiple cells without requiring an external force.[6] CNSAs are comprised of vertically oriented nanoscale syringes made of carbon deposited nanoporous anodized aluminum oxide (AAO). CNSAs have an interesting design in that they contain an empty compartment for cargo loading, a feature distinct from other NW structures. An enhanced GFP-expressing plasmid loaded onto CNSAs was delivered to NIH3T3 cells, which then displayed 34% enhanced GFP positive cells, as measured by flow cytometry. Both plasmid and quantum dots were delivered to human mesenchymal stem cells, and efficient delivery was observed in both cases. SEM images presented healthy NIH3T3 cells, which were widely spread over the surface of the CNSA.

Diamond nanoneedles were developed to mechanically breach the cell membrane and deliver macromolecules in the suspension into cells by diffusion.[22,27,28] Diamond, due to its high mechanical toughness, ensures the mechanical strength of nanoneedles with nanometer scale. Additionally, diamond is chemically inert and biocompatible, features allowing its

safe application to cells. The distal tip diameter was 135 ± 20 nm; the base diameter was 1.6 ± 0.31 μm, and the length was 7.42 ± 1.35 μm. The delivery was studied by applying an A549 cell suspension to the diamond nanoneedle array in a culture medium containing luminescent iridium(III) polypyridine complex.[28] Additionally, cisplatin, an anticancer drug, was delivered, and a 39.9 ± 6.5% cell viability drop was observed due to the anticancer activity of cisplatin.[28]

Synthesis—The MWNT can be prepared by the standard arc-discharge technique, where a DC current is applied across two high-purity graphite electrodes in 500 Torr of Helium gas.[29] After periodic arc discharging, MWNTs were deposited onto the cathode. Although the arc-discharge method mostly produces MWNTs, single-walled CNTs can also be generated with the addition of various metal catalysts, such as Fe, Ni, or Co on a graphite cathode.[30] After transferring CNTs between two metallic electrodes, they can be aligned under the AC signal applied between electrodes.[31] An SEM electron beam was applied at the junction between the CNT and AFM tip surface to weld the CNT onto the AFM tip.[32,33] Streptavidin-coated quantum dots were loaded with the fabricated MWNT-AFM tip by noncovalent complexation of streptavidin.[5]

A CNSA can be produced by a nanoporous template. The overall fabrication process of CNSAs is depicted in Figure 4.[6] The procedure was comprised of four main steps: (1) fabrication of nanoporous AAO, (2) carbon deposition inside the AAO by the thermal CVD method at 600 °C, (3) Ar ion milling and chemical etching (i.e., solution of phosphoric acid, chromic acid, and DI water) to release the CNSA, and (4) coating of an amphiphilic polymer by immersing the nanotubes in the amphiphilic polymer solution to convert the hydrophobic surface to a hydrophilic exterior for cargo loading.[6] The CNSAs were loaded with either the plasmids or quantum dots in water, and cells were placed on top.[6]

The diamond nanoneedles can be fabricated by deposition of a nanodiamond film using microwave plasma CVD on an n-type Si wafer followed by the RIE process.[28,34] After growing 2–8 μm-thick nanodiamond films,[28,35] RIE was conducted with molybdenum particles, which were self-sputtered from a substrate holder and acted as etching masks.[36,37]

Cell Toxicity—An MTT (3-(4,5-dimethylthiazol-2-yl)-2,5-diphenyltetrazolium bromide) assay displayed that the treated cells had a significantly increased viability (more than 85%) compared to the lipofectamine-transfected control cells.[6]

2.3. Nanostraw

The lack of control over temporal and spatial molecular release has been a long-standing challenge of the field. In an attempt to address this challenge, the Melosh group developed nanostraw platforms that establish continuous fluidic access to cells using hollow nanostructures that can penetrate cells (Figure 5a).[11,27,38–40] Nanostraws were designed to achieve time-resolved and spatially controlled intracellular delivery of small molecules, genetic materials, and proteins. Cells cultured on small-diameter nanostraws (less than 100 nm) were spontaneously penetrated, and the holes created a stable access route to intracellular compartments that were sustained over a time period of days. Nanostraws allow for time-resolved and sequential delivery without the need for continuous cell penetration.[11]

Nanostraw devices are able to deliver molecules ranging from ions to DNA plasmids with subminute temporal resolution. Alexa 488 dye delivered using a nanostraw resulted in homogeneous fluorescence in the cytoplasm that is clearly different from the fluorescent punctate formed in the cells after Alexa 568 treatment into the upper culture well, as seen in Figure 5b and c.[11] These contrasting patterns suggest that there is a principal difference in the nanostraw dye delivery mechanism compared to extracellular dye uptake.[11] The same group improved the nanostraw platform by applying a short duration (20 to 200 μs electrical pulses) electric field with a low voltage (5 to 20 V) across the membrane (Figure 5d).[39]

The addition of an electric field improved the transfection efficiency up to 81%, a significant increase compared to the 10% efficiency observed in the control that was not subjected to an electric field. Efficient deliveries were achieved for both dye (>95%) and plasmid transfections (~81%) into HEK 293T cells (plasmid transfection ~67%) and Chinese hamster ovary cells, all with cell viability higher than 98%.[39] Additional experiments showing dose-controlled cotransfection (simultaneous transfection with two or more separate plasmid DNA) and sequential transfection demonstrate that the nanoelectroporation system is a versatile platform for transfecting cells in high-throughput.[39]

Synthesis—The fabrication of a nanostraw begins with a track-etched polycarbonate membrane with a pore size of 100–250 nm.[11,38,39] The porous membrane was then coated with alumina by atomic layer deposition, and a plasma RIE process followed this to remove the alumina layer on the top surface of the polycarbonate membrane.[11,38,39] Finally, the polycarbonate membrane was anisotropically etched by oxygen plasma to expose the alumina straw.[11,38,39] The fabricated nanostraw membrane was placed on top of a polydimethylsiloxane (PDMS) microfluidic channel and permanently bonded by oxygen plasma treatment.[11,38,39] A GFP plasmid was delivered by introducing certain concentrations of plasmid into the microchannel underneath the nanostraw membrane (Figure 5a).[11]

Mechanism—The Melosh group studied the mechanism of nanostraw delivery using a transparent platform to quantitatively analyze the kinetics and spatial locations of high-aspect nanostraws penetrating the cell membrane.[38] A transparent platform with nanostraws was developed on top of a PDMS microfluidic chip to allow for high-resolution imaging of cells that are penetrated by nanostraws. Co^{2+} quenching and ethylene-diamine-tetra-acetic acid recovery were conducted sequentially with precise temporal control to understand the delivery mechanism. Xu et al. found that a low number of cells (6–12%) were actually penetrated by nanostraws.[38] However, further observation revealed that once the nanostraws did penetrate the cell, they maintain sustained intracellular access. Actin and adhesion proteins were locally accumulated around the nanostraw, indicating a potential method for downstream signaling.[38]

Cell Toxicity—The mRNA expression profiles of cells cultured on nanostraws were tested to understand their effect on cellular function and gene expression. Low-density nanostraws presented a minor effect on gene expression levels with slightly reduced levels compared to those of the control.[11] The long-term cell viability was also studied for nanostraw-electroporated cells. The results showed that cell viability was up to 98% for 3 days after

electroporation (20 V/200 μs/200 pulses), comparable results of cells cultured without electroporation conditions.[39] Moreover, the study found that the density of nanostraws was also important for nanostraw applications, as high-density arrays of nanostraws (>10^9/cm^2) did not allow cells to adhere to the structure and be penetrated.[11,41]

2.4. Nanoengineered Particles

The high-aspect ratio of NWs on a particle creates unique properties useful for macromolecule delivery purposes. The Desai group created a nanoengineered microparticle (NEMP) on which conformal Si NWs were coated.[15,42–44] Figure 6 depicts the structure and SEM images of NEMPs.[15,43] The Si NWs in the NEMP system offer two unique features: a large drug loading area in a hollow reservoir between the Si NWs and a unique nanostructure that enhances effective adhesion to mucus.[15,43] NW structures provide a high-level of adhesion as it physically sticks to the mucus layer. Many different types of nanoengineered particles with various shapes have been developed for efficient in vitro or in vivo delivery of macromolecules.[14,16,42,45,46]

Tetrapods with high-aspect ratio nanotips were developed by Nie et al.[25] The unique structure of zinc oxide (ZnO) tetrapods was designed to deliver plasmid DNA concurrently to prevent penetration of the whole structure due to its geometric hindrance. Furthermore, the structure ensures that the spikes are exposed to cells, allowing for efficient delivery with low toxicity.[25] Amino-modified ZnO tetrapods loaded with GFP expressing plasmid were delivered to A375 cells and achieved efficiency comparable to lipofectamine transfection. An advantage of this technology is that ZnO tetrapods can be treated on cells that have already been plated and are in the process of being cultured on regular dishes, whereas many other mechanical delivery methods cannot be applied under these circumstances.[25] The ability to apply this method on cells already plated and cultured is advantageous because it minimizes the toxicity and perturbation issues frequently raised in other methods requiring a cell detachment step.

Synthesis—NEMPs were prepared from 30–50 μm glass microspheres and controlled pore glass particles (30–70 μm, 200 nm pore size).[43] Si NWs were conformally grown on the particles using standard VLS deposition, and protein was loaded by surface absorption.[43] The tetrapod-like ZnO nanostructures can be directly synthesized by thermal evaporation of metal zinc under atmospheric pressure.[25] A few spherical zinc pellets were rapidly heated in a quartz tube at 900 °C for 2 min. The white fog, the cluster of tetrapod-like ZnO nanostructures that formed inside the tube, was then collected and dispersed in ethanol. The purity of nanostructures can be further improved by adjusting the oxygen concentration in the carrier gas at 1100 °C.[47] The fabricated tetrapod-like ZnO nanostructures were mixed with a solution of 2-propanol and ethanol.[25] Deionized water and ammonia solution were added. Tetrapods modified with APTES and tetraethylorthosilicate were mixed with enhanced GFP plasmid to prepare the silica-coated and amino-modified tetrapod-like ZnO nanostructures.[25] Plasmid loading was achieved with reversible electrostatic interactions of DNA and amino groups coated on the tetrapods.[25]

Cell Toxicity—For determination of cytotoxicity of the ZnO tetrapods, an MTT assay was conducted and 80–90% viability with respect to the control was observed, which is a significantly higher viability compared to lipofectamine transfected cells.[25] However, a potential drawback of these particle systems is that removal of the nanostructured particles from the cells after macromolecule delivery can be challenging. Therefore, in-depth cytotoxicity analysis and methods to remove the particles from pierced cells are required for application of the technology.

3. IN VIVO APPLICATIONS

High-aspect ratio nanotopography has also been studied for its use related to in vivo applications.[27,48] A recent study presented that nanostructured microneedles increased the transdermal delivery efficiency of etanercept, a 150 kDa protein therapeutic for autoimmune diseases including rheumatoid arthritis, in both rats and rabbits.[16] Chiappini et al. presented that porous Si NNs delivered quantum dots to muscle and skin in mice.[10] Quantum dots were found in confined areas associated with the surface layer in which nanoinjection was conducted, and they stayed in the area for up to 100 h.[10] Transmission electron microscopy images proved the presence of quantum dots in the cytosolic region of cells from a target region.[10] Additionally, VEGF165 plasmid DNA was delivered using nanoneedles and induced higher expression of human VEGF165 compared to direct injection, and the effect was sustained for up to 7 days.[9] Nanoneedle delivery of VEGF enhanced vascularization and increased the levels of blood perfusion and the number of nodes 6-fold, which are important indicators of neovascularization.[9] Additionally, Peng et al. demonstrated that Si NW arrays, using a modular self-assembled synthetic approach and DNA nanoparticles, can deliver plasmids by transplantation of the arrays.[49] The combination of cyclodextrin-grafted branched PEI, adamantane-grafted polyamidoamine, adamantine-grafted poly(ethylene glycol, PEG), and Si NWs achieved efficient delivery of DNA supramolecular nanoparticles in mice.[49]

Another preferred drug delivery method is through mucosal tissues, which are the primary absorptive interfaces for the uptake of therapeutics. However, these tissues have numerous chemical and physical defensive barriers, such as degradative enzymes, harsh pH conditions, tight junctions, and a mucus layer to prevent the entry of unwanted substances.[14,44,50,51] The mucus layer has a quick turnover time of 50–170 min to clear substances that do not directly interact with the cells.[51,52] Because of the viscous and motile nature of the mucus, therapeutic macromolecules take a longer time to diffuse into cells, increasing their susceptibility to degradation and removal.[50] The Desai group developed nanowire-coated systems to overcome the challenge of mucus layer protection.[14,15,45] NEMPs increase retention time up to 10-fold more than that of unmodified particles and improve device adhesion in vivo, as shown in Figure 7.[15] NEMPs were maintained in the stomach for 120 min and showed increased retention in the large intestine by 180 min.[15] A recent study presented that nanoengineered planar particles provide a much higher drug-loading efficiency compared to spherical particles due to their larger surface area.[14] Most planar particles adhere to cells with their largest faces, thus increasing the transepithelial permeation of insulin while simultaneously loosening the tight junctions of epithelial cells.[14]

NEMPs were used to deliver insulin orally, and this resulted in significantly increased blood insulin levels.[14]

4. EFFECTS OF NANOSTRUCTURES ON CELL PHYSIOLOGY

Nanoscale topographical structures provide physical cues to cells and have been shown to influence various cell responses.[53–57] Recent studies suggest that the key determinants of cell behavior include both interactions with environmental structures and physical cues.[46,58,59] Specifically, nano-scale high-aspect ratio structures have been shown to induce mechanotransduction and enhance the drug delivery profile.

Tight Junctions

Tight junctions are apical intercellular structures in epithelial and endothelial cells that function as the paracellular barrier. Tight junctions keep constitutive cells cohesive and polarized by structurally supporting the epithelium and determining the kinetics of the permeation of molecules across the cell layer.[44,60] Tight junctions in the gastrointestinal tract have 1–3 nm in pore size, which is too small a gap for most of macromolecules and conventional polymers to permeate.[42] Therefore, methods to widen intercellular junctions and enable paracellular delivery of drugs across the epithelial barrier have been extensively investigated.[16]

The effect of NWs on enhancing tight junction permeability by mechanotransduction was displayed with many high-aspect ratio nanostructures.[6,14,42] NEMPs added to Caco-2 cells in culture lead to alterations in tight junction permeability, localization of ZO-1 and f-actin, and decreased width of zonula occludens-1 (ZO-1) and claudin-1 at the tight junction.[14] NWs on NEMPs cause increased drug permeability in proportion to the amount of NWs added to the cell and enable more efficient paracellular transfer of the drug across the intestinal epithelial barrier.[42] Interestingly, the mechanical effect from the stiff Si NWs was mitigated by soft PEG shielding.[42] PEGylated NEMPs reduced permeability due to their increased inertness in comparison to the nonfunctionalized NWs and beads, and as a result, did not increase the flux of the drug across the epithelial layer.[42]

Size Selective Delivery

Enhanced permeability by NEMPs depends on the size of drug being delivered. Small molecules such as fluorescein (332 Da) are able to readily cross the epithelium without requiring the aid of nanostructures due to their tiny size. Peptide or small protein drugs, such as insulin (5.6 kDa) and FITC-dextran (4 kDa), were selectively delivered only with the assistance of NEMPs. In the case of larger molecules, such as FITC-dextran (10 kDa) and FITC-IgG (150 kDa), NEMPs were unable to facilitate their transport across the membrane.[14] The result indicates that facilitated delivery by mechanotransduction is selective to small macromolecules with a size less than 10 kDa.[14] A recent study showed that even large proteins, like FITC-BSA, FITC-IgG, and etanercept (Mw = 150 kDa), can be delivered in a facilitated manner across the epithelial barrier exposed to a nanostructured thin film.[45] Subsequent studies have discovered that tight junction proteins, such as occludins, ZO-1,

and claudins, participate in a mechanotransduction mechanism that is induced by nanostructures.[14,16,42,44,45]

Mechanism

Recent studies propose an integrin signaling mechanism to explain the enhanced paracellular permeability produced by nanostructured films. The expression of myosin light chain (MLC) kinase, a tight junction related protein kinase that contacts the cortical actin cytoskeleton, was significantly increased in cells, which are in contact with the nanostructured films. The expression levels of these cells were 5.6- and 19-fold larger than that of cells in contact with the unimprinted films and untreated controls, respectively.[16,45] Integrin binding to the nanotopography and phosphorylation of the MLC allowed tight junction proteins to be remodeled.[16] Figure 8 demonstrates that the tight junction protein ZO-1 was under morphological changes due to its interaction with the nanostructured thin film.[45] As a result, the actomyosin complex was activated and the mechanotransduction pathways increased paracellular permeability.[16,45] In addition, an MTT assay showed an insignificant difference in cell viability between control cells and the nanostructured film-treated cells.[45]

5. CONCLUSIONS AND OUTLOOK

In this review, recent advances of in vitro and in vivo physical delivery of macromolecules by high-aspect ratio nanostructures were summarized with the synthesis methods, material properties, and applications. For in vitro applications, the high-aspect ratio nanostructures, including silicon nanowires, carbon nanotubes, diamond nanoneedles, nanostraws, and nanoengineered particles, have addressed many challenges present in conventional methods, such as cell membrane passage and endosomal degradation, and showed the feasibility of efficient and high-throughput macromolecule delivery with minimal perturbation of cells. For in vivo applications, high-aspect ratio nanotopography has improved transdermal delivery of plasmids and etanercept as well as the device adhesion time by overcoming the challenge of numerous chemical and physical defensive barriers, such as degradative enzymes, tight junctions, and mucus layer protection.

Recent studies have presented the possibility of a high-throughput monolithic platform to delivery various macromolecules into a wide variety of cell types.[2,10,13] The physical delivery methods using nanostructures are efficient, especially with primary cells which are notoriously hard to transfect using conventional methods. Moreover, the nanostructure-assisted delivery methods are free from viral packaging or chemical modifications, thus making the delivery process simple to scale up. Many of the nanostructures are suitable for multiplexing and microarray technology, key steps for high-throughput analysis.[6,13] In addition, microfluidics platforms with nanostructures will allow simplified optimization of the customized nanostructures for numerous different cell types and delivery cargos. Microfluidics platforms will also allow the process to be quicker and more efficient with minimal cell perturbation. Recent advances in the organ-on-a-chip field allow for various types of cell culture on a chip and the formation of tissue in conditions that very closely mimic physiological conditions. The organ-on-a-chip systems allow for primary cell culture in a physiologically relevant environment. The systems have displayed the potential for easy

drug screening of small molecules. We anticipate that nanostructures will enable the systems to deliver macromolecules to cell cultures on the chip and also allow for genetic or intracellular protein screening of macromolecular therapeutics. The application can open doors to a new era of personalized medication with the combination of organ-on-a-chip and high-throughput nanostructure-assisted delivery systems. In vivo applications of the nanostructures are also expected to expand the range of applications of nanostructures in medicine. In addition, high-aspect ratio nanostructures have a variety of uses in theranostics, containing the potential to conduct both diagnosis and treatment with a single device. We anticipate that high-aspect ratio nanostructures have a vast potential to impact a broad range of high-throughput screening applications in science and medicine.

Acknowledgments

This work was supported by grants from the NIH, U01 268201000043C-0-0-1, RO1 AI107116-01, and RO1 AI088023-03. In addition, this work was supported by the Siebel Scholars Foundation and the WM Keck Foundation. We thank Professors Luke P. Lee and Tejal A. Desai for inspiration and advice.

References

1. Sharei A, Zoldan J, Adamo A, Sim WY, Cho N, Jackson E, Mao S, Schneider S, Han MJ, Lytton-Jean A, Basto PA, Jhunjhunwala S, Lee J, Heller DA, Kang JW, Hartoularos GC, Kim KS, Anderson DG, Langer R, Jensen KF. A Vector-free Microfluidic Platform for Intracellular Delivery. Proc Natl Acad Sci U S A. 2013; 110:2082–2087. [PubMed: 23341631]
2. Shalek AK, Robinson JT, Karp ES, Lee JS, Ahn DR, Yoon MH, Sutton A, Jorgolli M, Gertner RS, Gujral TS, MacBeath G, Yang EG, Park H. Vertical Silicon Nanowires as a Universal Platform for Delivering Biomolecules into Living Cells. Proc Natl Acad Sci U S A. 2010; 107:1870–1875. [PubMed: 20080678]
3. Lee K, Rafi M, Wang X, Aran K, Feng X, Lo Sterzo C, Tang R, Lingampalli N, Kim HJ, Murthy N. In Vivo Delivery of Transcription Factors with Multifunctional Oligonucleotides. Nat Mater. 2015; 14:701–706. [PubMed: 25915034]
4. Lee K, Yu P, Lingampalli N, Kim HJ, Tang R, Murthy N. Peptide-enhanced mRNA Transfection in Cultured Mouse Cardiac Fibroblasts and Direct Reprogramming towards Cardiomyocyte-like Cells. Int J Nanomed. 2015; 10:1841–1854.
5. Chen X, Kis A, Zettl A, Bertozzi CR. A Cell Nanoinjector based on Carbon Nanotubes. Proc Natl Acad Sci U S A. 2007; 104:8218–8222. [PubMed: 17485677]
6. Park S, Kim YS, Kim WB, Jon S. Carbon Nanosyringe Array as a Platform for Intracellular Delivery. Nano Lett. 2009; 9:1325–1329. [PubMed: 19254005]
7. McAllister DV, Wang PM, Davis SP, Park JH, Canatella PJ, Allen MG, Prausnitz MR. Microfabricated Needles for Transdermal Delivery of Macromolecules and Nanoparticles: Fabrication Methods and Transport Studies. Proc Natl Acad Sci U S A. 2003; 100:13755–13760. [PubMed: 14623977]
8. Donnelly RF, Singh TRR, Woolfson AD. Microneedle-based Drug Delivery Systems: Microfabrication, Drug Delivery, and Safety. Drug Delivery. 2010; 17:187–207. [PubMed: 20297904]
9. Chiappini C, De Rosa E, Martinez JO, Liu X, Steele J, Stevens MM, Tasciotti E. Biodegradable Silicon Nanoneedles Delivering Nucleic Acids Intracellularly Induce Localized in Vivo Neovascularization. Nat Mater. 2015; 14:532–539. [PubMed: 25822693]
10. Chiappini C, Martinez JO, De Rosa E, Almeida CS, Tasciotti E, Stevens MM. Biodegradable Nanoneedles for Localized Delivery of Nanoparticles in Vivo: Exploring the Biointerface. ACS Nano. 2015; 9:5500–5509. [PubMed: 25858596]
11. VanDersarl JJ, Xu AM, Melosh NA. Nanostraws for Direct Fluidic Intracellular Access. Nano Lett. 2012; 12:3881–3886. [PubMed: 22166016]

12. Kim W, Ng JK, Kunitake ME, Conklin BR, Yang P. Interfacing Silicon Nanowires with Mammalian Cells. J Am Chem Soc. 2007; 129:7228–7229. [PubMed: 17516647]
13. Shalek AK, Gaublomme JT, Wang L, Yosef N, Chevrier N, Andersen MS, Robinson JT, Pochet N, Neuberg D, Gertner RS, Amit I, Brown JR, Hacohen N, Regev A, Wu CJ, Park H. Nanowire-Mediated Delivery Enables Functional Interrogation of Primary Immune Cells: Application to the Analysis of Chronic Lymphocytic Leukemia. Nano Lett. 2012; 12:6498–6504. [PubMed: 23190424]
14. Uskoković V, Lee K, Lee PP, Fischer KE, Desai TA. Shape Effect in the Design of Nanowire-Coated Microparticles as Transepithelial Drug Delivery Devices. ACS Nano. 2012; 6:7832–7841. [PubMed: 22900471]
15. Fischer KE, Nagaraj G, Daniels RH, Li E, Cowles VE, Miller JL, Bunger MD, Desai TA. Hierarchical Nanoengineered Surfaces for Enhanced Cytoadhesion and Drug Delivery. Biomaterials. 2011; 32:3499–3506. [PubMed: 21296409]
16. Walsh L, Ryu J, Bock S, Koval M, Mauro T, Ross R, Desai T. Nanotopography Facilitates in Vivo Transdermal Delivery of High Molecular Weight Therapeutics through an Integrin-Dependent Mechanism. Nano Lett. 2015; 15:2434–2441. [PubMed: 25790174]
17. Chan MS, Lo PK. Nanoneedle-Assisted Delivery of Site-Selective Peptide-Functionalized DNA Nanocages for Targeting Mitochondria and Nuclei. Small. 2014; 10:1255–1260. [PubMed: 24323905]
18. HochbaumaI, FanR, , HeR, , YangP. Controlled Growth of Si Nanowire Arrays for Device Integration. Nano Lett. 2005; 5:457–460. [PubMed: 15755094]
19. Fan R, Wu Y, Li D, Yue M, Majumdar A, Yang P. Fabrication of Silica Nanotube Arrays from Vertical Silicon Nanowire Templates. J Am Chem Soc. 2003; 125:5254–5255. [PubMed: 12720419]
20. Wu Y, Fan R, Yang P. Block-by-Block Growth of Single-Crystalline Si/SiGe Superlattice Nanowires. Nano Lett. 2002; 2:83–86.
21. Hulteen JC, Van Dyne RP. Nanosphere Lithography: A Materials General Fabrication Process for Periodic Particle Array Surfaces. J Vac Sci Technol, A. 1995; 13:1553–1558.
22. He B, Yang Y, Yuen MF, Chen XF, Lee CS, Zhang WJ. Vertical Nanostructure Arrays by Plasma Etching for Applications in Biology, Energy, and Electronics. Nano Today. 2013; 8:265–289.
23. Liu Y, Wu DC, Zhang WD, Jiang X, He CB, Chung TS, Goh SH, Leong KW. Polyethylenimine-Grafted Multiwalled Carbon Nanotubes for Secure Noncovalent Immobilization and Efficient Delivery of DNA. Angew Chem, Int Ed. 2005; 44:4782–4785.
24. Boussif O, Lezoualc'h F, Zanta MA, Mergny MD, Scherman D, Demeneix B, Behr JP. A Versatile Vector for Gene and Oligonucleotide Transfer into Cells in Culture and In Vivo: Polyethylenimine. Proc Natl Acad Sci U S A. 1995; 92:7297–7301. [PubMed: 7638184]
25. Nie L, Gao L, Yan X, Wang T. Functionalized Tetrapod-like ZnO Nanostructures for Plasmid DNA Purification, Polymerase Chain Reaction and Delivery. Nanotechnology. 2007; 18:015101.
26. Yum K, Na S, Xiang Y, Wang N, Yu MF. Mechanochemical Delivery and Dynamic Tracking of Fluorescent Quantum Dots in the Cytoplasm and Nucleus of Living Cells. Nano Lett. 2009; 9:2193–2198. [PubMed: 19366190]
27. Yan L, Zhang J, Lee CS, Chen X. Micro- and Nanotechnologies for Intracellular Delivery. Small. 2014; 10:4487–4504. [PubMed: 25168360]
28. Chen X, Zhu G, Yang Y, Wang B, Yan L, Zhang KY, Lo KKW, Zhang W. A Diamond Nanoneedle Array for Potential High-Throughput Intracellular Delivery. Adv Healthcare Mater. 2013; 2:1103–1107.
29. Ebbesen TW, Ajayan PM. Large-Scale Synthesis of Carbon Nanotubes. Nature. 1992; 358:220–222.
30. Shi Z, Lian Y, Zhou X, Gu Z, Zhang Y, Iijima S, Zhou L, Yue KT, Zhang S. Mass-Production of Single-Wall Carbon Nanotubes by Arc Discharge Method. Carbon. 1999; 37:1449–1453.
31. Chen XQ, Saito T, Yamada H, Matsushige K. Aligning Single-Wall Carbon Nanotubes with an Alternating-Current Electric Field. Appl Phys Lett. 2001; 78:3714–3716.

32. Martinez J, Yuzvinsky TD, Fennimore AM, Zettl A, García R, Bustamante C. Length Control and Sharpening of Atomic Force Microscope Carbon Nanotube Tips Assisted by an Electron Beam. Nanotechnology. 2005; 16:2493–2496.
33. Yu MF, Lourie O, Dyer MJ, Moloni K, Kelly TF, Ruoff RS. Strength and Breaking Mechanism of Multiwalled Carbon Nanotubes Under Tensile Load. Science. 2000; 287:637–640. [PubMed: 10649994]
34. Zou YS, Ma KL, Zhang WJ, Ye Q, Yao ZQ, Chong YM, Lee ST. Fabrication of Diamond Nanocones and Nanowhiskers by Bias-Assisted Plasma Etching. Diamond Relat Mater. 2007; 16:1208–1212.
35. Zhang WJ, Wu Y, Wong WK, Meng XM, Chan CY, Bello I, Lifshitz Y, Lee ST. Structuring Nanodiamond Cone Arrays for Improved Field Emission. Appl Phys Lett. 2003; 83:3365–3367.
36. Ando Y, Nishibayashi Y, Kobashi K, Hirao T, Oura K. Smooth and High-Rate Reactive Ion Etching of Diamond. Diamond Relat Mater. 2002; 11:824–827.
37. Ando Y, Nishibayashi Y, Sawabe A. 'Nano-Rods' of Single Crystalline Diamond. Diamond Relat Mater. 2004; 13:633–637.
38. Xu AM, Aalipour A, Leal-Ortiz S, Mekhdjian AH, Xie X, Dunn AR, Garner CC, Melosh NA. Quantification of Nanowire Penetration into Living Cells. Nat Commun. 2014; 5:3613. [PubMed: 24710350]
39. Xie X, Xu AM, Leal-Ortiz S, Cao Y, Garner CC, Melosh NA. Nanostraw–Electroporation System for Highly Efficient Intracellular Delivery and Transfection. ACS Nano. 2013; 7:4351–4358. [PubMed: 23597131]
40. Angle MR, Cui B, Melosh NA. Nanotechnology and Neurophysiology. Curr Opin Neurobiol. 2015; 32:132–140. [PubMed: 25889532]
41. Popat KC, Leoni L, Grimes CA, Desai TA. Influence of Engineered Titania Nanotubular Surfaces on Bone Cells. Biomaterials. 2007; 28:3188–3197. [PubMed: 17449092]
42. Uskoković V, Lee PP, Walsh LA, Fischer KE, Desai TA. PEGylated Silicon Nanowire Coated Silica Microparticles for Drug Delivery across Intestinal Epithelium. Biomaterials. 2012; 33:1663–1672. [PubMed: 22116000]
43. Fischer KE, Jayagopal A, Nagaraj G, Daniels RH, Li EM, Silvestrini MT, Desai TA. Nanoengineered Surfaces Enhance Drug Loading and Adhesion. Nano Lett. 2011; 11:1076–1081. [PubMed: 21280638]
44. Fox CB, Kim J, Le LV, Nemeth CL, Chirra HD, Desai TA. Micro/nanofabricated Platforms for Oral Drug Delivery. J Controlled Release. 2015; doi: 10.1016/j.jconrel.2015.07.033
45. Kam KR, Walsh LA, Bock SM, Koval M, Fischer KE, Ross RF, Desai TA. Nanostructure-Mediated Transport of Biologics across Epithelial Tissue: Enhancing Permeability via Nanotopography. Nano Lett. 2013; 13:164–171. [PubMed: 23186530]
46. Fox CB, Kim J, Schlesinger EB, Chirra HD, Desai TA. Fabrication of Micropatterned Polymeric Nanowire Arrays for High-Resolution Reagent Localization and Topographical Cellular Control. Nano Lett. 2015; 15:1540–1546. [PubMed: 25639724]
47. Li QH, Wan Q, Chen YJ, Wang TH, Jia HB, Yu DP. Stable Field Emission from Tetrapod-like ZnO Nanostructures. Appl Phys Lett. 2004; 85:636–638.
48. Yan L, Yang Y, Zhang W, Chen X. Advanced Materials and Nanotechnology for Drug Delivery. Adv Mater. 2014; 26:5533–5540. [PubMed: 24449177]
49. Peng J, Garcia MA, Choi JS, Zhao L, Chen KJ, Bernstein JR, Peyda P, Hsiao YS, Liu KW, Lin WY, Pyle AD, Wang H, Hou S, Tseng HR. Molecular Recognition Enables Nanosubstrate-Mediated Delivery of Gene-Encapsulated Nanoparticles with High Efficiency. ACS Nano. 2014; 8:4621–4629. [PubMed: 24708312]
50. Fox CB, Chirra HD, Desai TA. Planar Bioadhesive Microdevices: a New Technology for Oral Drug Delivery. Curr Pharm Biotechnol. 2014; 15:673–683. [PubMed: 25219863]
51. Fischer KE, Alemán BJ, Tao SL, Daniels RH, Li EM, Bünger MD, Nagaraj G, Singh P, Zettl A, Desai TA. Biomimetic Nanowire Coatings for Next Generation Adhesive Drug Delivery Systems. Nano Lett. 2009; 9:716–720. [PubMed: 19199759]
52. Lehr CM, Poelma FGJ, Junginer HE, Tukker JJ. An Estimate of Turnover Time of Intestinal Mucus Gel Layer in the Rat in situ Loop. Int J Pharm. 1999; 70:235–240.

53. Liu D, Yi C, Wang K, Fong CC, Wang Z, Lo PK, Sun D, Yang M. Reorganization of Cytoskeleton and Transient Activation of Ca^{2+} Channels in Mesenchymal Stem Cells Cultured on Silicon Nanowire Arrays. ACS Appl Mater Interfaces. 2013; 5:13295–13304. [PubMed: 24308382]

54. Yim EKF, Reano RM, Pang SW, Yee AF, Chen CS, Leong KW. Nanopattern-Induced Changes in Morphology and Motility of Smooth Muscle Cells. Biomaterials. 2005; 26:5405–5413. [PubMed: 15814139]

55. Dalby MJ, Gadegaard N, Tare R, Andar A, Riehle MO, Herzyk P, Wilkinson CDW, Oreffo ROC. The Control of Human Mesenchymal Cell Differentiation using Nanoscale Symmetry and Disorder. Nat Mater. 2007; 6:997–1003. [PubMed: 17891143]

56. Teo BKK, Wong ST, Lim CK, Kung TYS, Yap CH, Ramagopal Y, Romer LH, Yim EKF. Nanotopography Modulates Mechanotransduction of Stem Cells and Induces Differentiation through Focal Adhesion Kinase. ACS Nano. 2013; 7:4785–4798. [PubMed: 23672596]

57. Teo BKK, Goh SH, Kustandi TS, Loh WW, Low HY, Yim EKF. The Effect of Micro and Nanotopography on Endocytosis in Drug and Gene Delivery Systems. Biomaterials. 2011; 32:9866–9875. [PubMed: 21924770]

58. McBeath R, Pirone DM, Nelson CM, Bhadriraju K, Chen CS. Cell Shape, Cytoskeletal Tension, and RhoA Regulate Stem Cell Lineage Commitment. Dev Cell. 2004; 6:483–495. [PubMed: 15068789]

59. Engler AJ, Sen S, Sweeney HL, Discher DE. Matrix Elasticity Directs Stem Cell Lineage Specification. Cell. 2006; 126:677–689. [PubMed: 16923388]

60. Furuse M, Hata M, Furuse K, Yoshida Y, Haratake A, Sugitani Y, Noda T, Kubo A, Tsukita S. Claudin-based Tight Junctions are Crucial for the Mammalian Epidermal Barrier: a Lesson from Claudin-1–Deficient Mice. J Cell Biol. 2002; 156:1099–1111. [PubMed: 11889141]

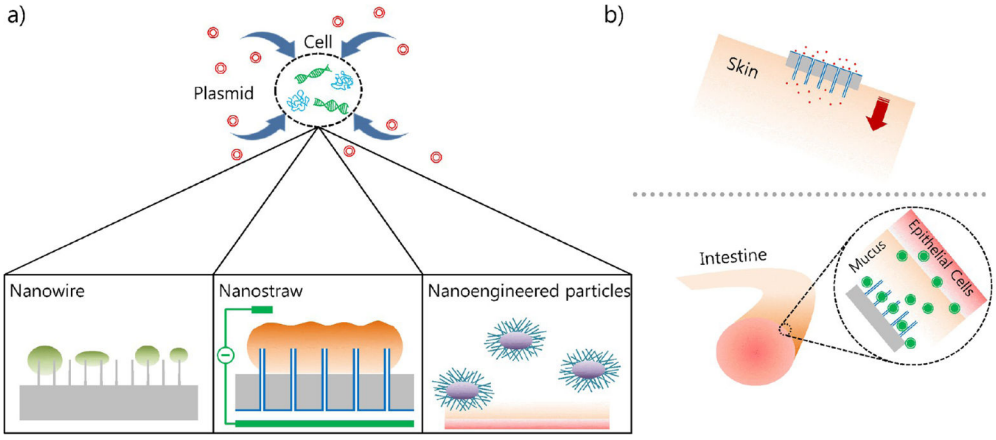

Figure 1.

Schematic of macromolecule delivery in (a) in vitro applications by high-aspect ratio nanostructured materials, including nanowires, nanostraws, and nanoengineered particles, and (b) in vivo applications.

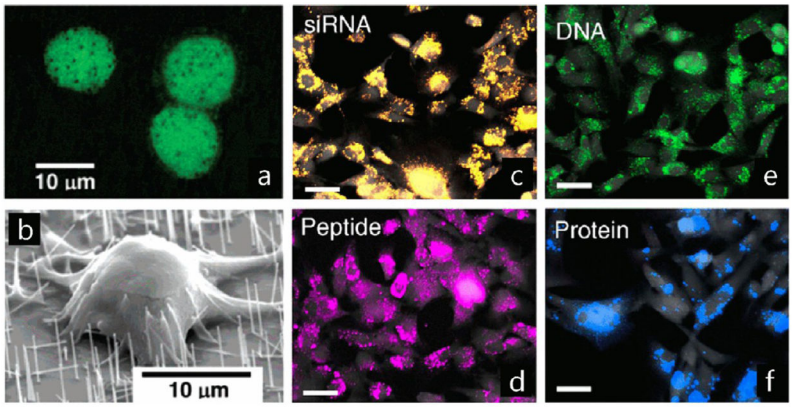

Figure 2.

Silicon nanowires (Si NW) deliver diverse macromolecules to cells by physical penetration. (a) Confocal microscopy image of mouse embryonic stem (mES) cells expressing GFP. Si NWs are shown as black dots in the cytoplasm. (b) SEM image of individual mES cells penetrated with Si NWs. (c–f) Fluorescence microscopy image of human fibroblasts transfected with various macromolecules. Cell were incubated on coated Si NWs for 24 h and replated on glass coverslips for imaging. Significant delivery was observed with (c) siRNA (Alexa Fluor 546-labeled negative control siRNA), (d) peptides (rhodamine-labeled 9-mer), (e) Cy5-labeled plasmid DNA, and (f) proteins (recombinant TurboRFP-mito). Scale bars: 50 μm for (c–f). Reproduced with permission from refs 2 and 12, copyright (2010) National Academy of Sciences and (2007) American Chemical Society, respectively.

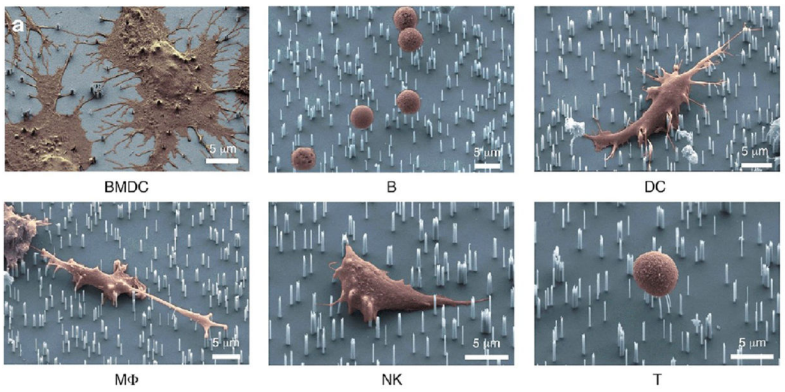

Figure 3.

Scanning electron microscope images demonstrate that various immune cells interact with silicon nanowires (Si NWs) in different ways. Primary immune cells were plated and incubated for 24 h on Si NWs plates (false colored blue): mouse bone-marrow dendritic cells (BMDCs), B cells, dendritic cells (DCs), macrophages (MΦs), natural killer (NK) cells, and T cells (false colored orange). Scale bar: 5 μm. Reproduced with permission from ref 13, copyright (2012) American Chemical Society.

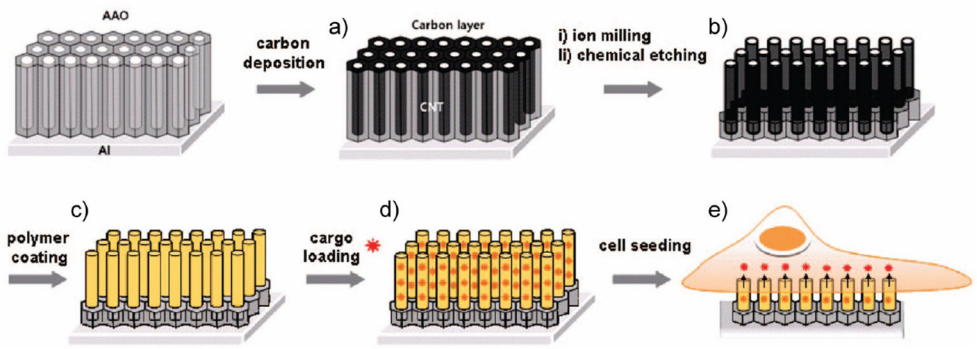

Figure 4.

Synthesis scheme of carbon nanosyringe arrays for cellular macromolecule delivery: (a) carbon layer deposition step using a thermal chemical vapor deposition method within the pore structure of a porous anodized aluminum oxide (AAO) template; (b) an ion milling step to remove the uppermost carbon surface from the AAO template and expose the carbon nanosyringes by chemical etching; (c) surface coating with amphiphilic polymer; (d) cargo loading; and (e) cell seeding and intracellular delivery. Reproduced with permission from ref 6, copyright (2009) American Chemical Society.

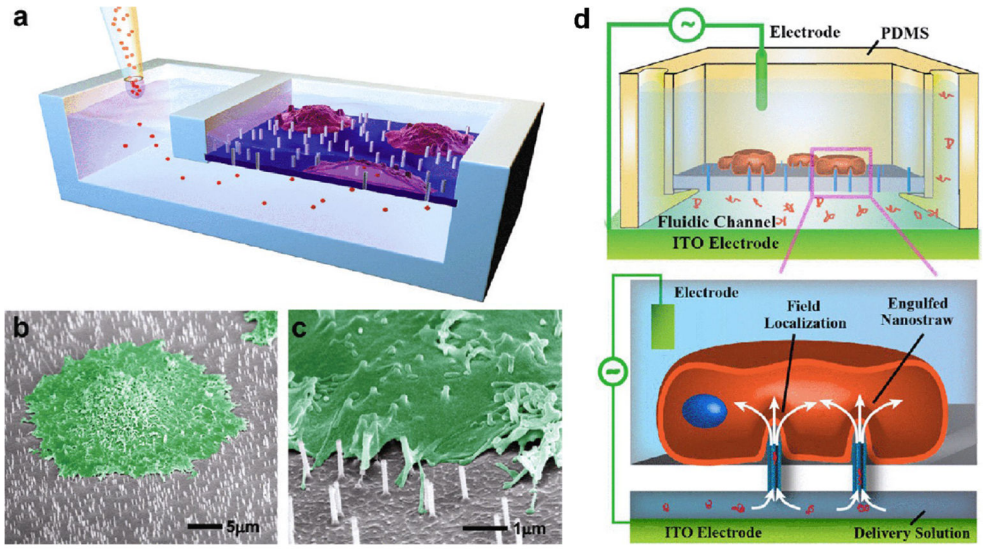

Figure 5.

Nanostraw works as a channel to an intracellular area. (a) Schematic illustration of nanostraw device. A cross section of the device shows macromolecule delivery by the nanostraw. (b, c) SEM images of critical point dried cells that were cultured on a nanostraw device with 100 nm diameter with high density. (d) Schematic illustrations of a nanostraw-electroporation system. Electric field is applied to facilitate macromolecule delivery. Reproduced with permission from refs 11 and 39, copyright (2012) and (2013) American Chemical Society, respectively.

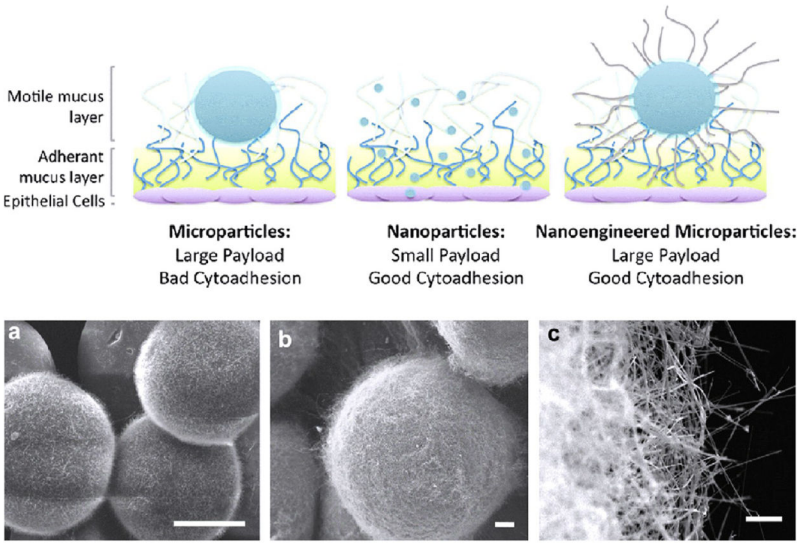

Figure 6.

Scheme and SEM images of nanoengineered particles. (a) silica spheres (30–50 μm diameter) with nanowires (1–3 μm in length and 40 nm in diameter). Scale bar indicates 20 μm. (b, c) Stainless steel spheres (200–220 μm) with nanowires (11 μm in length and 70 nm in diameter). Scale bar indicates 20 μm (b) and 2 μm (c). Reproduced with permission from refs 15 and 43, copyright (2011) Elsevier and (2011) American Chemical Society, respectively.

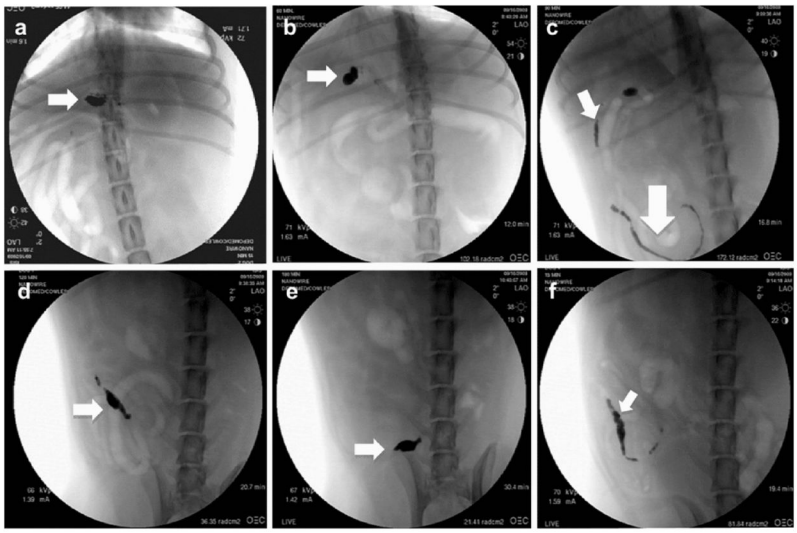

Figure 7.

In vivo X-ray images of nanowire-coated stainless steel devices orally administered to beagles. (a–f) Images of 200 μm devices at 15, 60, 90, 120, and 150 min, respectively. (a, b) Arrows indicate particles in the stomach. (c) Proximal and distal small intestine, and (d, e) and large intestine. (f) Corresponding position of uncoated control devices at 15 min in distal small intestine, which demonstrates much faster migration of uncoated devices compared to nanowire-coated devices. Reproduced with permission from ref 15, copyright (2011) Elsevier.

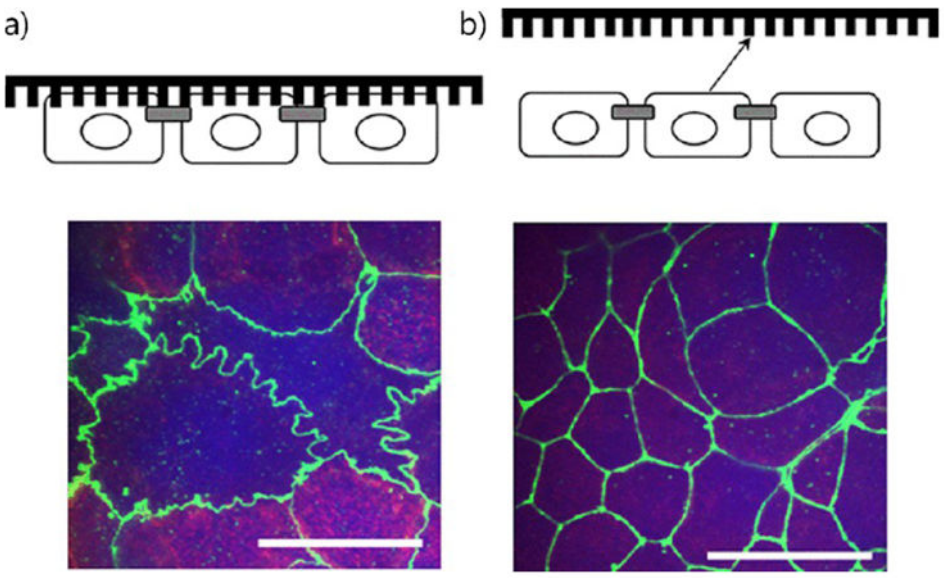

Figure 8.

Immunofluorescence staining of the tight junction protein zonula occluden (ZO-1) demonstrates that tight junctions go through morphological changes caused by the nanostructured thin film. (a) Nanostructured thin film induces a ruffled morphological change of tight junctions after 2 h, which indicates tight junction remodeling. (b) ZO-1 morphology recovered back to the normal architecture after nanostructured thin film removal, indicating that nanostructure-induced tight junction remodeling is reversible. Scale bar indicates 20 μm. Reproduced with permission from ref 45, copyright (2013) American Chemical Society.